Published in final edited form as:
Development. 2008 January ; 135(2): 271–280. doi:10.1242/dev.009688.

Eomesodermin, a target gene of Pou4f2, is required for retinal ganglion cell and optic nerve development in the mouse

Chai-An Mao[1], **Takae Kiyama**[1], **Ping Pan**[1], **Yasuhide Furuta**[1,2], **Anna-Katerina Hadjantonakis**[3], and **William H. Klein**[1,2,*]

[1]Department of Biochemistry and Molecular Biology, The University of Texas M. D. Anderson Cancer Center, Houston, TX 77030, USA

[2]Graduate Training Program in Genes and Development, The University of Texas Graduate School of Biomedical Sciences at Houston, Houston, TX 77030, USA

[3]Developmental Biology Program, Sloan-Kettering Institute, New York, NY 10021, USA

Summary

The mechanisms regulating retinal ganglion cell (RGC) development are crucial for retinogenesis and for the establishment of normal vision. However, these mechanisms are only vaguely understood. RGCs are the first neuronal lineage to segregate from pluripotent progenitors in the developing retina. As output neurons, RGCs display developmental features very distinct from those of the other retinal cell types. To better understand RGC development, we have previously constructed a gene regulatory network featuring a hierarchical cascade of transcription factors that ultimately controls the expression of downstream effector genes. This has revealed the existence of a Pou domain transcription factor, Pou4f2, that occupies a key node in the RGC gene regulatory network and that is essential for RGC differentiation. However, little is known about the genes that connect upstream regulatory genes, such as *Pou4f2* with downstream effector genes responsible for RGC differentiation. The purpose of this study was to characterize the retinal function of eomesodermin (Eomes), a T-box transcription factor with previously unsuspected roles in retinogenesis. We show that *Eomes* is expressed in developing RGCs and is a mediator of Pou4f2 function. Pou4f2 directly regulates *Eomes* expression through a *cis*-regulatory element within a conserved retinal enhancer. Deleting *Eomes* in the developing retina causes defects reminiscent of those in *Pou4f2*$^{-/-}$ retinas. Moreover, myelin ensheathment in the optic nerves of *Eomes*$^{-/-}$ embryos is severely impaired, suggesting that Eomes regulates this process. We conclude that Eomes is a crucial regulator positioned immediately downstream of Pou4f2 and is required for RGC differentiation and optic nerve development.

Keywords

Eomesodermin; T-box transcription factors; Pou4f2; Retinal ganglion cells; Optic nerve development; Mouse

Introduction

Among the six neuronal cell types in the vertebrate retina, retinal ganglion cells (RGCs) are the sole output neurons conveying visual information into the brain. RGCs are also the first

*Author for correspondence (whklein@mdanderson.org).

Supplementary material: Supplementary material for this article is available at http://dev.biologists.org/cgi/content/full/135/2/271/DC1

retinal cell type to differentiate. These features distinguish RGCs from the other retinal cell types and emphasize the importance of elucidating the mechanisms that regulate RGC development in order to create a comprehensive, integrated model of retinogenesis.

In the mouse, differentiating RGCs can first be visualized with molecular markers as early as embryonic day 11.5 (E11.5) when dividing retinal progenitor cells (RPCs) cease mitosis and migrate basally from the neuroblast side of the retinal epithelium towards the vitreal side to the emerging ganglion cell layer (GCL) (Young, 1985a; Young, 1985b). We and others have investigated the mechanisms controlling RGC fate specification and differentiation, and by doing so, have identified key regulatory factors that are essential for these events to occur normally (for reviews, see Mu and Klein, 2004; Mu and Klein, 2008; Cayouette et al., 2006). In particular, we have proposed a gene regulatory network model for RGC development featuring a hierarchical cascade of transcription factors that ultimately controls the expression of terminal downstream effector genes (Mu et al., 2005). Two transcription factors occupy key nodes in the RGC gene regulatory network: the proneural bHLH transcription factor Math5 (Atoh7 – Mouse Genome Informatics) and the class IV Pou domain-containing transcription factor Pou4f2 (also called Brn3b). Math5 is responsible for endowing RPCs with the competence to acquire a RGC fate (Brown et al., 2001; Wang et al., 2001), whereas Pou4f2 is positioned genetically downstream of Math5 and is essential for RGC differentiation, cell survival, neurite outgrowth and axon pathfinding (Erkman et al., 1996; Erkman et al., 2000; Gan et al., 1996; Gan et al., 1999; Wang et al., 2000). Notably, RGCs that lack Pou4f2 are still able to differentiate, albeit abnormally, and the expression of many RGC genes is refractory to the absence of Pou4f2 (Mu et al., 2004). This suggests that pathways operate in parallel along with Pou4f2 to control RGC differentiation (Mu et al., 2004; Mu et al., 2005).

For our RGC gene regulatory network model to be meaningful, connections must be made between individual upstream regulatory genes such as *Pou4f2* to terminal downstream genes such as those that control axon projections. Unfortunately, with the exception of *Pou4f1* (Trieu et al., 1999), little is known about regulatory genes that might be direct targets of Pou4f2. We therefore sought to determine whether any genes encoding transcription factors downstream of Pou4f2 are direct Pou4f2 targets, and whether these transcription factors mediate the roles played by Pou4f2 in regulating genes involved in terminal differentiation events. We focused on the eomesodermin (*Eomes*) gene for the following reasons. *Eomes* (also referred to as *Tbr2*) belongs to the *Tbr1*/*Eomes*/*Tbet* subfamily of genes (Naiche et al., 2005) that were initially found to play essential roles during trophoblast and mesoderm development in mice (Russ et al., 2000; Strumpf et al., 2005). *Eomes* is also expressed in the developing central nervous system and has been implicated in the development of the human central nervous system; a homozygous breakpoint mutation in a Moroccan family silences *Eomes* and leads to microcephaly (Baala et al., 2007). Recent studies have also indicated that Eomes is a component of a pathway that regulates glutamatergic neurogenesis in the cerebral cortex and cerebellum in mouse development (Bulfone et al., 1999; Hevner et al., 2006; Quinn et al., 2007). Of particular interest from the standpoint of our studies, *Eomes* was also found to be expressed in the GCL of the retina (http://www.scripps.edu/cb/friedlander/gene_expression/), prompting us to hypothesize that *Eomes* plays a role in RGC differentiation.

In this study, we extend the initial findings on *Eomes* in the developing retina by providing evidence that *Eomes* is a direct target of Pou4f2, and by demonstrating a role for *Eomes* in RGC differentiation and optic nerve development. We also discovered a novel role for *Eomes*: that it regulates myelin ensheathment in the developing optic nerve.

Materials and Methods

Generation of *Eomes*$^{flox/flox}$ mice and *Eomes-enhancer* transgenic embryos

A gene targeting vector was constructed containing a floxed *Eomes* allele in which exon 3 of *Eomes* could be deleted by Cre-mediated recombination. We used genomic DNA from R1 embryonic stem (ES) cells to PCR amplify 1.63, 0.45 and 2.79 kb fragments from the *Eomes* locus containing coding exons 1-5 and associated introns (see Fig. 6A). The amplified products were sequentially subcloned into a targeting vector generated previously in our laboratory (C.A.M., unpublished). The final targeting construct contained two *loxP* sites inserted into the second and third introns and a *PGK-neomycin* cassette with flanking *Frt* sites inserted into intron 3 adjacent to the *loxP* site (see Fig. 6A). The targeting construct was linearized and electroporated into ES cells, after which G418-resistant ES cells were selected to identify homologous recombination events. Targeted ES cell clones were identified by Southern analysis (see Fig. 6B). Chimeric males were bred to wild-type C57/BL/6J females to generate *Eomes*$^{+/flox}$ heterozygotes. To delete the *Frt-neomycin* cassette, we bred *Eomes*$^{+/flox}$ mice with mice containing a *Rosa26-FLPeR* transgene (Farley et al., 2000). *Eomes*$^{flox/flox}$ homozygous mice were obtained by interbreeding against the C57BL/6J background. *Eomes*$^{flox/flox}$ mice were viable and fertile.

A *CMV-Cre* transgenic line was used to generate *Eomes*$^{+/\Delta flox}$ in one-cell zygotes (Su et al., 2002). We then interbred *Eomes*$^{+/\Delta flox}$ mice to recover *Eomes*$^{\Delta flox/\Delta flox}$ embryos, which displayed phenotypes identical to those observed in germline-generated *Eomes*$^{-/-}$ embryos (Russ et al., 2000). To delete exon 3 in the developing retina, *Eomes*$^{+/flox}$ mice were bred to the *Six3-Cre* transgenic line, which expresses *Cre* in neural progenitor cells in the retina (Furuta et al., 2000). The resulting *Eomes*$^{+/flox}$*;Six3-Cre* males were bred to *Eomes*$^{flox/flox}$ females to generate *Eomes*$^{flox/flox}$*;Six3-Cre* embryos and neonates in which exon 3 was specifically deleted in the retina (*Eomes*$^{\Delta flox/\Delta flox}$*;Six3-Cre*).

Three PCR primers were used simultaneously to distinguish wild-type, floxed and deleted *Eomes* alleles (see Fig. 6C): Em15, 5′-CATGATTAAGGAAGGCTGGATGCAC-3′; Em16, 5′-AAGGAGACAGCCTTCACCCAGGC-3′; and Em18, 5′-GACTGAGAAGTAAGAGGGTCAGCAG-3′. PCR primers used to genotype the *Six3-Cre* transgene were Cre01, 5′-AACGAGTGATGAGGTTCGCAAGAAC-3′, and Cre02, 5′-CGCTATTTTCCATGAGTGAACGAACC-3′.

To generate embryos carrying the *Eomes-enhancer* transgene, a 2.8 kb region from base pairs −1182 to −3918 (translational start site, +1) of *Eomes* was subcloned into a plasmid containing the *hsp68-lacZ-pA* reporter gene (Kothary et al., 1989). The *Eomes-enhancer* transgene was used to generate transgenic embryos, which were collected at the desired times.

The US Public Health Service Policy on Humane Care and Use of Laboratory Animals was followed in all experiments using mice, and the M. D. Anderson Institutional Animal Care and Use Committee approved all animal protocols used in these experiments.

Histology studies, in situ hybridization, immunohistochemistry and X-gal staining

Embryos and eyes dissected from embryos or animals were fixed, paraffin-embedded and sectioned into 7 μm or 12 μm slices for immunohistochemistry studies or in situ hybridization, respectively (Mu et al.,2004). After de-waxing and rehydration, the sections were stained with Hematoxylin and Eosin for histology studies. In situ hybridization was performed as described by Mu et al. (Mu et al., 2004).

For the immunohistochemistry studies, sections were placed in a microwave oven at 600 watts in 10 mM sodium citrate for 18 minutes to expose the antigen epitopes. Microwave-treated

sections were then incubated with primary antibodies. A tyromide signal amplification kit (TSA biotin system, PerkinElmer) was used in conjunction with a NovaRed kit (Vector Labs), to detect Eomes protein expression by color, and the immunostained sections were counterstained with Methyl Green. To detect Eomes expression using indirect immunofluorescence, we used the TSA plus fluorescence kit to optimize the signal intensity. For double-immunofluorescence labeling, Eomes expression was detected as described above and the expression of all other proteins was detected using Alexa-conjugated secondary antibodies (Invitrogen). The primary antibodies were anti-BrdU (Upstate, 1/4), anti-Brn3b/Pou4f2 (Santa Cruz, 1/200), anti-GFP (Invitrogen, 1/1000), anti-NFL (Invitrogen, 1/250), anti-syntaxin (Chemicon, 1/1000), anti-Tbr1 (Chemicon, 1/1000) and anti-Tbr2/Eomes (Chemicon, 1/1000). HRP-conjugated secondary antibody for tyromide signal amplification was obtained from Jackson ImmunoResearch. Flat-mount retinas were prepared as described by Xiang et al. (Xiang et al., 1995).

TUNEL assays and BrdU labeling

TUNEL assays on embryonic retinas were performed using an in situ cell death detection kit (Roche Applied Science) following the manufacturer's instructions. Three paraffin-embedded sections were used for data analysis. For pulse labeling with BrdU, 100 μg of BrdU (Upstate) per gram of body weight was injected intraperitoneally into pregnant females 1 hour before euthanization. Embryos were then processed as described previously by Fu et al. (Fu et al., 2006).

Chromatin immunoprecipitation and electrophoretic mobility shift assays

E15.5 retinas were isolated for chromatin immunoprecipitation (ChIP) assays following the procedures described by Wells and Farnham (Wells and Farnham, 2002) and Kiyama and Klein (Kiyama and Klein, 2007). Two microliters of the immunoprecipitated chromatin DNA and input genomic DNA were used for PCR amplification with the following primer sets: Eo3b007, 5′-GACCAACTTGCCACAAAAAACCC-3′ and Eo3b008, 5′-CTGAACAGGCTTGCTGCATGCTC-3′; or TTN E4F, 5′-TTGCAGCAACCACTCTTGTC-3′ and TTN E4R, 5′-GCATGATGGGAGAGGACCTA-3′. PCR amplifications were performed for 30 cycles. The amplified products were resolved by 6% polyacrylamide gel electrophoresis and visualized by staining with GelStar nucleic acid gel stain (CAMBREX).

Electrophoretic mobility shift assays (EMSAs) were performed as described by Mu et al. (Mu et al., 2004). Oligonucleotides for the wild-type and mutated site A (see Fig. 4A) were: wild-type, 5′-GGGAGTGCTGGTGACCCGTTAATGTTGGAATGTTTTCCTA-3′ and mutant, 5′-GGGAGTGCTGGTGACCCGAAAAAGTTGGAATGTTTTCCTA-3′. Pou4f2 protein was synthesized in vitro using a transcription/translation system (Promega), and 2 μl of the transcription/translation reaction mixture was used for each EMSA reaction.

Cell cultures, DNA transfections, and lacZ reporter gene assays

U2OS cells were cultured in 10% Dulbecco's modified Eagle's medium and 10% fetal bovine serum at 37°C in a 5% CO_2 atmosphere. For the Eo2.8k (A^mB^m)-HSP68p-LacZ-pA plasmid, the core Pou4f2 binding site A was changed from 5′-GTTAATGTT-3′ to 5′-GAAAAAGTT-3′ and site B was changed from 5′-ATTAATGAG-3′ to 5′-AAAAATGTG-3′ using the Quikchange site-directed mutagenesis kit (Stratagene). Full-length Pou4f2 cDNA was subcloned into pIRES-hrGFP-1a (Stratagene) for transactivation experiments. Transfections were carried out on cover slides placed in six-well culture plates using FuGene HD (Roche) following the manufacturer's instructions. Cells were co-transfected with 0.5 μg of the *Pou4f2* expression construct or the empty expression vector and 0.5 μg of the reporter plasmid. X-gal staining was performed 36 hours after transfection. Transfection efficiency was

determined by visually inspecting the number of *GFP*-expressing cells for each experiment. All experiments were performed in triplicate.

Results

Spatiotemporal pattern of *Eomes* expression in the developing retina

We determined the spatial and temporal pattern of *Eomes* transcripts in the retina at E14.5 and E16.5 using sectioned in situ hybridization. At E14.5, the first signs of *Eomes* expression in the retina were mainly in the GCL, although cells within the neuroblast layer (NBL) were sparely labeled (Fig. 1A). At E16.5, *Eomes* continued to be expressed in the GCL and NBL (Fig. 1B). We also found *Eomes* to be strongly expressed in the forebrain, a previously known site of *Eomes* expression (Bulfone et al., 1999) (Fig. 1B). To determine whether *Eomes* is expressed at stages earlier than E14.5, we performed immunohistochemistry with anti-Eomes antibody in sections obtained at E13.5. Although Eomes protein was readily detected in the forebrain at this stage, it was not detected in the retina (Fig. 1C).

Because the GCL consists of displaced amacrine cells as well as RGCs, it was possible that *Eomes* was expressed in either both or one of these neuronal cells types. To test these possibilities, we performed immunohistochemistry in sections of wild-type and *Math5*$^{-/-}$ retinas obtained at E16.5. Retinas of *Math5*$^{-/-}$ embryos lack RGCs and in their place are increased numbers of displaced amacrine cells (Wang et al., 2001). Although wild-type retinas strongly expressed *Eomes* in the GCL, *Eomes* expression in *Math5*$^{-/-}$ retinas was virtually undetectable (Fig. 1D,E). These results demonstrated that RGCs in the GCL are the major site of *Eomes* expression from E14.5 to E16.5, a time when newly forming RGCs are populating the GCL.

Pou4f2 is one of the earliest markers of RGC differentiation (Gan et al., 1999) and is expressed in newly forming RGCs within the NBL and in differentiated RGCs that have migrated to the GCL (Gan et al., 1999). By comparing Pou4f2 and Eomes protein expression, we determined how much the expression of the two transcription factors overlapped and their potential relationship to each other. Although Eomes expression was not detected in retinas at E13.5 (Fig. 1C), Pou4f2 was already expressed at high levels at this time (Gan et al., 1999). By E14.5, Eomes expression was apparent and coincided with the existence of a subset of Pou4f2-expressing cells within the GCL (Fig. 1F-H). However, many Pou4f2-expressing cells, particularly those still migrating to the GCL, did not express Eomes. In addition, although Pou4f2 was expressed in RGCs throughout the GCL, Eomes was not expressed in the peripheral-most region (Fig. 1H). This would be in keeping with the fact that neuronal differentiation begins at the center and advances to the periphery of the retina. At E16.5, expression of Pou4f2 was largely confined to the GCL and many, but not all, of the Pou4f2-expressing cells also expressed Eomes (Fig. 1I-K). These results suggested that RGCs increasingly express Eomes as they migrate to the GCL and undergo terminal differentiation.

Weaker expression of Eomes within the NBL at E14.5 and E16.5 did not overlap with the expression of Pou4f2 and persisted throughout retinogenesis. As cells within the NBL are a mixture of mitotically active RPCs and newly formed postmitotic cells that have left the cell cycle and committed to a retinal cell fate (Le et al., 2006), we determined whether Eomes was expressed in mitotic cells by pulse-labeling S-phase cells of the E18.0 retinas with BrdU and comparing the relative distributions of the S-phase cells and Eomes-expressing cells. We detected little, if any, overlap between these two cell populations (Fig. 2A-C), suggesting that Eomes-expressing cells are mainly postmitotic.

We also observed that retinal Eomes expression persisted into postnatal life. In particular, *Eomes* was observed to be strongly expressed in the GCL and in the innermost region of the

emerging inner nuclear layer (INL) of newborn mice (P0) (Fig. 2D). Weaker expression was observed throughout the NBL (Fig. 2D). However, Eomes expression was largely absent in the GCL but persisted in the INL and NBL of retinas of newly born *Math5*$^{-/-}$ mice (Fig. 2E). Because amacrine cells are the major cell type in the innermost region of the INL, it is possible that the Eomes-expressing cells were amacrine cells and that the Eomes-expressing cells in the NBL were amacrine cell progenitors.

At P12, Eomes expression was detected in a subpopulation of cells in the GCL, where its expression co-localized with that of the RGC marker neurofilament light subunit (NFL) (Fig. 2F). At P30, Eomes expression in the INL co-localized with that of the pan-amacrine cell marker syntaxin (Fig. 2G) but not of other amacrine cell markers calbindin and parvalbumin (data not shown). A few Eomes-expressing cells in the INL were found to be colocalized with the amacrine marker calretinin (data not shown). These results suggested that Eomes-expressing cells in the INL constituted a distinct subpopulation of amacrine cells.

Identification of a phylogenetically conserved *Eomes* retinal enhancer

Because Pou4f2 is expressed in newly arising RGCs and is required for RGC differentiation, *Eomes* might be positioned genetically downstream of *Pou4f2*, making it a potential target gene of Pou4f2. If this were the case, *Eomes* expression would necessarily depend on the presence of functional Pou4f2. To test this possibility, we determined the level of Eomes protein expression in retinas isolated from *Pou4f2*$^{+/-}$ (wild type) and *Pou4f2*$^{-/-}$ embryos. We performed the analysis at E14.5 because *Pou4f2*$^{-/-}$ retinas have the same number of RGCs as wild-type retinas at that stage. *Eomes* expression in the GCL strictly depended on Pou4f2; Eomes protein in the GCL was undetectable in *Pou4f2*$^{-/-}$ retinas but clearly detectable in *Pou4f2*$^{+/-}$ control littermates (Fig. 3A,B).

These results indicated that *Eomes* is genetically downstream of Pou4f2 but they did not show whether Pou4f2 is directly involved in regulating *Eomes* transcription. We therefore determined whether conserved noncoding sequences containing Pou4f2 consensus DNA-binding sites [5′-(A/G)TTAATGAG(C/T)-3′; Xiang et al. (Xiang et al., 1995)] could be identified within the *Eomes* locus. We focused our search on a 20 kb stretch of genomic DNA that encompasses the *Eomes* gene along with 9.5 kb of DNA upstream of the *Eomes* translational initiation codon and 4.1 kb of DNA downstream of the *Eomes* translational termination codon. By comparing human, mouse, rat and dog genomes, we identified several blocks of conserved noncoding sequences that were located within the upstream and downstream DNA sequences flanking *Eomes* (Fig. 3C). Furthermore, two putative Pou4f2-binding sites were identified in two closely separated regions. One site (site B, Fig. 3C,D) began at base pair −2937 (5′-ATTAATGAG-3′) and its sequence precisely matched that of the consensus Pou4f2-binding site. The other site (site A, Fig. 3C,D) began at base pair −3854 (5′-GTTAATGTT-3′) and differed from another Pou4f2-binding site by one base pair. However, Pou4f2-binding site B was not conserved in the corresponding position in human, rat and dog genomes (Fig. 3D). By contrast, Pou4f2-binding site A was located within a highly conserved 192 bp region (Fig. 3D), and this site was present in all four vertebrate genomes with the exception of one mismatched nucleotide in the dog genome.

To determine whether the conserved upstream regions containing the Pou4f2-binding sites were capable of directing expression in the developing retina, we constructed a transgene containing a 2.8 kb fragment that included both Pou4f2-binding sites fused to an hsp68-promoter-*lacZ*-pA reporter gene (Fig. 3E). The resultant transgenic E14.5 embryos expressed *lacZ* in retinas and limbs, a previously known region of *Eomes* expression (Russ et al., 2000) (Fig. 3E). In control experiments, a transgene construct with disabling mutations in sites A and B did not express in either the limb or retina (data not shown). In the wild-type construct, *lacZ* was expressed in a narrow strip within the inner part of the retina just above the GCL

(Fig. 3F). β-Galactosidase-stained retinal sections co-stained with anti-Eomes antibody, showed that most of the *lacZ*-expressing cells did not co-express the endogenous Eomes protein (compare Fig. 3A with 3F). A possible explanation for the lack of overlap is that the *lacZ*-expressing cells represent newly forming RGCs in the process of migrating to the GCL. To determine whether this was the case, we performed immunohistochemistry analysis of β-galactosidase-stained retinal sections from E14.5 transgenic embryos using anti-Brn3b (Pou4f2) antibody. From these experiments, it was clear that most of the *lacZ*-expressing cells also expressed Pou4f2, although Pou4f2 expression was present in many cells that were not expressing the transgene (Fig. 3G). These results demonstrated that the 2.8 kb fragment is sufficient to direct transgene expression in a subpopulation of RGCs and that this subpopulation also expresses Pou4f2. However, the transgene appeared to be expressed at earlier stages in RGC differentiation than the stages when endogenous Eomes is expressed. The reason why transgene and Eomes expression do not correlate is uncertain, but it suggests that crucial *cis*-regulatory elements are missing in the 2.8 kb region. Consistent with this, a 225 kb Bac transgenic mouse line containing *Eomes* fused to an eGFP reporter (Bac Eomes::GFP) (Kwon and Hadjantonakis, 2007) expresses *GFP* in the GCL of E14.5 and E16.5 retinas in a manner similar to that of endogenous *Eomes* expression (Fig. 3H-K).

To determine whether either Pou4f2-binding sites A or B within the 2.8 kb fragment bind to Pou4f2, we used EMSA to detect Pou4f2 binding in vitro and ChIP to detect Pou4f2 binding in vivo. EMSA was performed using an in vitro-synthesized full-length Pou4f2 protein and an oligonucleotide probe containing the putative Pou4f2-binding site A within the conserved 192 bp region. We detected a specific Pou4f2-DNA complex but no complex was formed with transcription-translation lysates that lacked the Pou4f2 template (Fig. 4A). The formation of the Pou4f2-DNA complex was inhibited when excess homologous unlabeled oligonucleotide competitor but not when excess oligonucleotide competitor containing a mutated Pou4f2 site was added. Addition of the anti- Pou4f2/Brn3b antibody also blocked complex formation (Fig. 4A). Notably, an oligonucleotide competitor containing the Pou4f2-binding site B did not interfere with complex formation, suggesting that this nonconserved sequence was not a bona fide Pou4f2-binding site.

ChIP analysis was performed using chromatin prepared from E15.5 retinas and primer pairs that would reveal Pou4f2 bound to the Pou4f2-binding site within the conserved 192 bp region. This showed that a 122 bp fragment was amplified after immunoprecipitation with anti-Brn3b antibody (Fig. 4B), but not with preimmune IgG, which served as a negative control (data not shown). In addition, sequences derived from the gene encoding the muscle-specific protein Titin were not immunoprecipitated with anti-Brn3b antibody (Fig. 4B). We also performed ChIP experiments using anti-acetylated-histone H3 antibody to determine whether the Pou4f2-binding site was within a region of open (acetylated) chromatin, a finding that would indicate active expression. The 122 bp fragment was also amplified after immunoprecipitation with anti-acetylated-histone H3 antibody, whereas sequences from the gene encoding Titin were not (Fig. 4B). Both the Pou4f2-binding site and Titin sequences were amplified after immunoprecipitation with anti-histone H3 antibody, which ubiquitously marks the presence of nucleosomes (Fig. 4B). These results implicate Pou4f2 as a direct transcription regulator of *Eomes* expression acting at the Pou4f2-biding site A within the conserved 192 bp region. A similar ChIP analysis was performed using the nonconserved Pou4f2-binding site B. A very weak PCR product was observed when primer pairs were used that amplified a 157 bp fragment containing the putative Pou4f2 site B (data not shown). This result was consistent with the view that the nonconserved Pou4f2 site B is likely to have only a minor function, if any, in vivo.

To provide further evidence that Pou4f2 is a transcriptional regulator of *Eomes*, we performed transient transactivation assays in U2OS cells using the 2.8 kb fragment-*lacZ* reporter gene

construct containing Pou4f2-binding sites A and B (see Fig. 3E). A control construct, Eo2.8K (A^mB^m)-HSP68p-LacZ-pA, was generated in which binding sites A and B were mutated. The number of cells expressing *lacZ* was sharply increased when the wild-type construct was co-transfected with the *Pou4f2* expression plasmid (Fig. 5A,B), with little increase in the number of cells with the mutated construct (Fig. 5C,D). These results demonstrate that Pou4f2 is able to activate transcription from the 2.8 kb fragment and suggest that Pou4f2-binding to site A, and to a lesser extent site B, enhances *Eomes* transcription in RGCs.

Abnormal RGC and optic nerve development in *Eomes*$^{\Delta flox/\Delta flox}$ retinas

To assess the role of *Eomes* in the developing retina, we generated mice with a floxed allele of *Eomes* and bred them with a *Six3-Cre* transgenic mouse line to delete exon 3 of *Eomes* in the developing retina (Fig. 6). Histological retinal sections of *Eomes*$^{\Delta flox/\Delta flox}$ mice at P24 showed a slight reduction in the thickness of the GCL compared with *Eomes*$^{+/flox}$ controls, whereas the INL and ONL were normal (Fig. 7A,B). This suggests that in the absence of *Eomes*, the RGCs are reduced in number and that they possess other defects as well.

To visualize the RGC axons, we prepared flat mounts of retinas that were immunohistochemically stained with anti-NFL antibody. In *Eomes*$^{\Delta flox/\Delta flox}$ P30 retinas, we observed ~30% reduction in the number of RGC axons in both the central and peripheral regions of the retina when compared with *Eomes*$^{+/flox}$ retinas (Fig. 7C-F). The density of the axon bundles was also notably reduced, and their orientation towards the optic disk appeared abnormal (arrowheads, Fig. 7F). The reduction in the number of RGCs and the defects associated with RGC axons associated with *Eomes*$^{\Delta flox/\Delta flox}$ retinas were similar to those identified in *Pou4f2*$^{-/-}$ retinas, although the overall effects appeared less severe in *Eomes*$^{\Delta flox/\Delta flox}$ retinas.

As RGCs undergo enhanced apoptosis between E15.5 and E18.5 in *Pou4f2*$^{-/-}$ retinas (Gan et al., 1999), we performed a TUNEL analysis of sectioned retinas from *Eomes*$^{+/flox}$ and *Eomes*$^{\Delta flox/\Delta flox}$ embryos and postnatal mice to look for differences in apoptosis patterns between the two. Although there was no significant enhancement of apoptosis through E16.5 (data not shown), at E18.5 we detected a dramatic increase in apoptotic cells in *Eomes*$^{\Delta flox/\Delta flox}$ retinas in both the GCL and NBL with respect to *Eomes*$^{+/flox}$ retinas (arrowheads, Fig. 7G-J). At P1, P6 and P12, the number of apoptotic cells was consistently higher in *Eomes*$^{\Delta flox/\Delta flox}$ retinas than in *Eomes*$^{+/flox}$ controls, but the differences were less dramatic than they were at E18. (Fig. 7I,J). Apoptotic cells were also observed in the GCL, INL and ONL. We did not observe significant differences between *Eomes*$^{\Delta flox/\Delta flox}$ retinas and *Eomes*$^{+/flox}$ controls after P12. These results suggest that the reduced number of RGCs that we observed in the retinas of P30 *Eomes*$^{\Delta flox/\Delta flox}$ mice resulted from the enhanced apoptosis of RGCs within the GCL between E18 and P12. However, the reason for increased cell death in the retinal NBL, INL and ONL of embryos and postnatal *Eomes*$^{\Delta flox/\Delta flox}$ mice is uncertain. Some of the apoptotic cells might represent the Eomes-positive amacrine cells and their progenitors that weakly expressed *Eomes* in the NBL at earlier stages.

As the expression of *Eomes* in RGCs correlated with the time when RGC axons reach the optic chiasm, this raised the possibility that *Eomes* might play a role in regulating some aspects of RGC axon formation. To assess this possibility, we isolated optic nerves from adult *Eomes*$^{\Delta flox/\Delta flox}$ and *Eomes*$^{+/flox}$ mice, and examined their ultrastructure (Wang et al., 2000). In a section about 0.5 cm from the optic disk, a region where mature RGC axons are well myelinated and ensheathed, low-magnification TEM showed that the area of *Eomes*$^{\Delta flox/\Delta flox}$ optic nerves was 30% smaller than that of *Eomes*$^{+/flox}$ optic nerves (Fig. 8A,B), consistent with the finding that RGC numbers were reduced by ~30%. At higher magnifications, we observed striking differences between *Eomes*$^{\Delta flox/\Delta flox}$ and *Eomes*$^{+/flox}$ optic nerves (Fig. 8C,D). In particular, the axons in the optic nerves of *Eomes*$^{+/flox}$ mice were ensheathed with a well-

organized, compact myelinated layer. However, only a few axons in the optic nerves of *Eomes*$^{\Delta flox/\Delta flox}$ mice were myelinated and where present, myelin ensheathment was thinner, disorganized and loosely packed (Fig. 8C, parts iii-vi, Fig. 8D, parts iii-vi). Moreover, in the optic nerves of *Eomes*$^{\Delta flox/\Delta flox}$ mice, we observed neurites that were smaller in diameter than those of normal axons and that contained large numbers of microtubules rather than the neurofilaments normally associated with RGC axons in the optic nerve (arrowheads, Fig. 8D, part vi). This finding was highly reminiscent of the abnormalities we observed in the optic nerves of *Pou4f2*$^{-/-}$ mice reported earlier (Wang et al., 2000). Because we had not in that study determined whether myelination was abnormal in *Pou4f2*$^{-/-}$ optic nerves, we performed a similar TEM analysis in *Pou4f2*$^{-/-}$ mice. We found, indeed, that there were similar defects in myelination and ensheathment in *Pou4f2*$^{-/-}$ mice (data not shown), providing additional evidence that Eomes mediates the functions of Pou4f2 in RGC and optic nerve development.

Discussion

In this study, we found that *Eomes* is expressed in differentiated RGCs within the GCL but not in committed progenitors or newly forming RGCs within the NBL. We further observed that *Eomes* expression begins when *Pou4f2* expression is maximal and depends on Pou4f2. Our results therefore provide evidence that *Eomes* is a direct target gene of Pou4f2. We also found that a 2.8 kb fragment upstream of *Eomes*, which encompasses a highly conserved 192 bp region that contains a Pou4f2-binding site, directs RGC expression in transgenic embryos. Furthermore, Pou4f2 binds efficiently to and activates transcription from this site. Analysis of *Eomes*$^{\Delta flox/\Delta flox}$ retinas indicated that *Eomes* plays roles similar to but more restricted than that of *Pou4f2* in RGC differentiation, cell survival and optic nerve development. Overall, our results argue strongly for our hypothesis that *Eomes* is positioned immediately downstream of *Pou4f2* and is a mediator, at least in part, of Pou4f2 function. Eomes, therefore, appears to be an important transcription factor that connects Pou4f2 to the expression of genes associated with terminal differentiation, particularly those involved in axon outgrowth and optic nerve development.

Eomes as a likely target gene of Pou4f2

When fused to a minimal promoter and a *lacZ* reporter transgene, a 2.8 kb fragment upstream of *Eomes* that contains several conserved noncoding sequence blocks directs reporter gene expression to a subpopulation of cells within the NBL that co-express *Pou4f2*. The fact that the cells expressing the transgene are in the NBL and that they also express *Pou4f2* strongly suggests that the cells are newly forming RGCs in the process of migrating from the NBL to the GCL. As transgene expression in the retina is highly restricted to these *Pou4f2*-expressing cells, this implies that *Eomes* expression is dependent on the presence of Pou4f2. However, endogenously expressed *Eomes* is clearly found in RGCs that also express *Pou4f2* but have already migrated to the GCL. Thus, the 2.8 kb fragment does not faithfully reproduce the endogenous expression pattern of *Eomes*. Nevertheless, retinal expression of the transgene is highly restricted to RGCs. A possible explanation for this is that additional cis-regulatory elements lying outside the 2.8 kb fragment modulate the spatiotemporal activity of *Eomes*. Indeed, a 225 kb Bac *Eomes-eGFP* transgene appears to recapitulate endogenous *Eomes* expression, suggesting that *Eomes* is regulated by multiple enhancer inputs, one of which is within the 2.8 kb region. In addition, non-deleted *Eomes* transcripts are downregulated in *Eomes*$^{\Delta flox/\Delta flox}$ retinas, suggesting that Eomes regulates its own expression (C.-A.M. and W.H.K., unpublished).

Eomes in RGC differentiation and retinal development

Major defects were observed in the retinas of *Eomes*$^{\Delta flox/\Delta flox}$ mice. This included reduced numbers of RGC, abnormal RGC axon outgrowth and an aberrant and disorganized myelin

sheath surrounding RGC axons. The massive cell death in the GCL associated with the loss of Eomes indicates that Eomes is required for the survival of at least some RGCs. Presumably, the absence of Eomes results in abnormal differentiation, which in turn triggers apoptosis. The increased number of apoptotic cells in other retinal layers might be associated with the weak expression of *Eomes* observed in non-RGCs or might be an indirect consequence of abnormal levels of apoptotic cells within the GCL.

One of the striking retinal defects in $Eomes^{\Delta flox/\Delta flox}$ embryos is the disorganized and loosely packed myelin sheaths surrounding RGC axons in the optic nerve. Axon ensheathment is essential for the normal propagation of membrane potential, and when defective, results in slow and continuous depolarization along the axon (Waxman et al., 1995). It is therefore likely that the propagation of visual signals into the brain is severely compromised in $Eomes^{\Delta flox/\Delta flox}$ mice. Because axon outgrowth and myelination require changes in the cell adhesion properties of axons (Bartsch, 2003), the abnormal ensheathment possibly has its source in defective cell adhesion. Many members of the T-box transcription factor family, including Eomes, are involved in regulating genes whose products are important for cell adhesion (Strumpf et al., 2005; Inman and Downs, 2006). Eomes acting downstream of Pou4f2 might therefore regulate the genes whose products are required for substrate adhesion.

T-box proteins in retinal development

Several members of the T-box transcription factor family besides Eomes are also expressed in retinal development. The vertebrate orthologs of the *Drosophila* gene *optomotor-blind*, *Tbx2*, *Tbx3* and *Tbx5*, are expressed early in the dorsal part of the developing retina and are thought to function in dorsoventral axial patterning (Pflugfelder et al., 1992; Sowden et al., 2001). In addition, *Tbx12* and *Tbx20* are expressed in the developing retina and Tbx12 is required for the formation of retinal cells and the organization of retinal layers (Carson et al., 2000; Carson et al., 2004; Kraus et al., 2001).

A conserved DNA-binding T-domain is found in all T-box transcription factors (Kispert and Herrmann, 1993; Bruneau et al., 2001; Conlon et al., 2001; Paxton et al., 2002; Wang et al., 2004) and a consensus T-box element is believed to be the binding site for all members of the T-box transcription factor family. Thus, it is possible that other T-box factors partially compensate for the loss of Eomes. To examine whether the absence of Eomes resulted in an upregulation of other T-box genes, which would be indicative of compensation, we determined the expression patterns of eight T-box genes in $Eomes^{+/flox}$ and $Eomes^{\Delta flox/\Delta flox}$ retinas. We were able to detect retinal expression of only *Trb1* and *Tbx5*, and no significant differences in expression were observed between $Eomes^{+/flox}$ and $Eomes^{\Delta flox/\Delta flox}$ retinas (see Fig. S1 in the supplementary material). It therefore seems likely that Eomes has evolved a specialized function in RGC development and is positioned in the RGC gene regulatory hierarchy downstream of Math5 and Pou4f2.

Supplementary Material

Refer to Web version on PubMed Central for supplementary material.

Acknowledgments

We thank Jan Parker-Thornburg, Chad Smith, the Genetically Engineered Mouse Facility, Kenneth Dunner, Jr, members of the High Resolution Electron Microscopy Facility and Jody Polan for advice and guidance on the confocal microscopy; Mathew Chempanal for technical support; and Xiuqian Mu for valuable input on the manuscript. These facilities, the DNA Analysis facility and the Research Animal Support Facility are supported in part by a National Institutes of Health-National Cancer Institute Comprehensive Cancer Center Support grant (CA16672). The work was supported by grants from the National Institutes of Health-National Eye Institute to W.H.K. (EY11930 and

EY010608-139005) and Y.F. (EY013128), and by the National Institute of Child Health and Human Development to K.H. (HD052115). We also acknowledge support from the Robert A. Welch Foundation (G-0010) to W.H.K.

References

Baala L, Briault S, Etchevers HC, Laumonnier F, Natiq A, Amiel J, Boddaert N, Picard C, Sbiti A, Asermouh A, et al. Homozygous silencing of T-box transcription factor EOMES leads to microcephaly with ploymicrogyria and corpus callosum agenesis. Nat Genet 2007;39:454–456. [PubMed: 17353897]

Bartsch U. Neural CAMS and their role in the development and organization of myelin sheaths. Front Biosci 2003;8:d477–d490. [PubMed: 12456309]

Brown NL, Patel S, Brzezinski J, Glaser T. Math5 is required for retinal ganglion cell and optic nerve formation. Development 2001;128:2497–2508. [PubMed: 11493566]

Bruneau BG, Nemer G, Schmitt JP, Charron F, Robitaille L, Caron S, Conner DA, Gessler M, Nemer M, Seidman CE, et al. A murine model of Holt-Oram syndrome defines roles of the T-box transcription factor Tbx5 in cardiogenesis and disease. Cell 2001;106:709–721. [PubMed: 11572777]

Bulfone A, Martinez S, Marigo V, Campanella M, Basile A, Quaderi N, Gattuso C, Rubenstein JL, Ballabio A. Expression pattern of the Tbr2 (Eomesodermin) gene during mouse and chick brain development. Mech Dev 1999;84:133–138. [PubMed: 10473127]

Carson CT, Kinzler ER, Parr BA. Tbx12, a novel T-box gene, is expressed during early stages of heart and retinal development. Mech Dev 2000;96:137–140. [PubMed: 10940636]

Carson CT, Pagratis M, Parr BA. Tbx12 regulates eye development in Xenopus embryos. Biochem Biophys Res Commun 2004;318:485–489. [PubMed: 15120626]

Cayouette M, Poggi L, Harris WA. Lineage in the vertebrate retina. Trends Neurosci 2006;29:563–570. [PubMed: 16920202]

Conlon FL, Fairclough L, Price BM, Casey ES, Smith JC. Determinants of T box protein specificity. Development 2001;128:3749–3758. [PubMed: 11585801]

Erkman L, McEvilly RJ, Luo L, Ryan AK, Hooshmand F, O'Connell SM, Keithley EM, Rapaport DH, Ryan AF, Rosenfeld MG. Role of transcription factors Brn-3.1 and Brn-3.2 in auditory and visual system development. Nature 1996;381:603–606. [PubMed: 8637595]

Erkman L, Yates PA, McLaughlin T, McEvilly RJ, Whisenhunt T, O'Connell SM, Krones AI, Kirby MA, Rapaport DH, Bermingham JR, et al. A POU domain transcription factor-dependent program regulates axon pathfinding in the vertebrate visual system. Neuron 2000;28:779–792. [PubMed: 11163266]

Farley FW, Soriano P, Steffen LS, Dymecki SM. Widespread recombinase expression using FLPeR (flipper) mice. Genesis 2000;28:106–110. [PubMed: 11105051]

Fu X, Sun H, Klein WH, Mu X. Beta-catenin is essential for lamination but not neurogenesis in mouse retinal development. Dev Biol 2006;299:424–437. [PubMed: 16959241]

Furuta Y, Lagutin O, Hogan BL, Oliver GC. Retina- and ventral forebrain-specific Cre recombinase activity in transgenic mice. Genesis 2000;26:130–132. [PubMed: 10686607]

Gan L, Xiang M, Zhou L, Wagner DS, Klein WH, Nathans J. POU domain factor Brn-3b is required for the development of a large set of retinal ganglion cells. Proc Natl Acad Sci USA 1996;93:3920–3925. [PubMed: 8632990]

Gan L, Wang SW, Huang Z, Klein WH. POU domain factor Brn-3b is essential for retinal ganglion cell differentiation and survival but not for initial cell fate specification. Dev Biol 1999;210:469–480. [PubMed: 10357904]

Hevner RF, Hodge RD, Daza RA, Englund C. Transcription factors in glutamaergic neurogenesis: conserved programs in neocortex, cerebellum, and adult hippocampus. Neurosci Res 2006;55:223–233. [PubMed: 16621079]

Inman KE, Downs KM. Brachyury is required for elongation and vasculogenesis in the murine allantois. Development 2006;133:2947–2959. [PubMed: 16835439]

Kispert A, Herrmann BG. The Brachyury gene encodes a novel DNA binding protein. EMBO J 1993;12:3211–3220. [PubMed: 8344258]

Kiyama T, Klein WH. SpGataE, a *Strongylocentrotus purpuratus* ortholog of mammalian Gata4/5/6: protein expression, interaction with putative target gene *spec2a*, and identification of friend of Gata factor SpFog1. Dev Genes Evol 2007;217:651–663. [PubMed: 17710433]

Kothary R, Clapoff S, Darling S, Perry MD, Moran LA, Rossant J. Inducible expression of an hsp68-lacZ hybrid gene in transgenic mice. Development 1989;105:707–714. [PubMed: 2557196]

Kraus F, Haenig B, Kispert A. Cloning and expression analysis of the mouse T-box gene tbx20. Mech Dev 2001;100:87–91. [PubMed: 11118890]

Kwon GS, Hadjantonakis AK. Eomes::GFP – a tool for live Imaging cells of the trophoblast, primitive streak, and telencephalon in the mouse embryo. Genesis 2007;45:208–217. [PubMed: 17417802]

Le TT, Wroblewski E, Patel S, Riesenberg AN, Brown NL. Math5 is required for both early retinal neuron differentiation and cell cycle progression. Dev Biol 2006;295:764–778. [PubMed: 16690048]

Mu X, Klein WH. A gene regulatory hierarchy for retinal ganglion cell specification and differentiation. Semin Cell Dev Biol 2004;15:115–123. [PubMed: 15036214]

Mu, X.; Klein, WH. Gene regulatory networks and the development of retinal ganglion cells. In: Chalupa, LM.; Williams, RW., editors. Eye, Retina, and Visual System of the Mouse. Cambridge, MA: MIT Press; 2008. In press

Mu X, Beremand PD, Zhao S, Pershad R, Sun H, Scarpa A, Liang S, Thomas TL, Klein WH. Discrete gene sets depend on POU domain transcription factor Brn4b/Brn-3.2/POU4f2 for their expression in the mouse embryonic retina. Development 2004;131:1197–1210. [PubMed: 14973295]

Mu X, Fu X, Sun H, Beremand PD, Thomas TL, Klein WH. A gene network downstream of transcription factor math5 regulates retinal progenitor cell competence and ganglion cell fate. Dev Biol 2005;280:467–481. [PubMed: 15882586]

Naiche LA, Harrelson Z, Kelly RG, Papaioannou VE. T-box genes in vertebrate development. Annu Rev Genet 2005;39:219–239. [PubMed: 16285859]

Paxton C, Zhao H, Chin Y, Langner K, Reecy J. Murine Tbx2 contains domains that activate and repress gene transcription. Gene 2002;283:117–124. [PubMed: 11867218]

Pflugfelder GO, Roth H, Poeck B, Kerscher S, Schwarz H, Jonschker B, Heisenberg M. The lethal (1) optomotor-blind gene of Drosophila melanogaster is a major organizer of optic lobe development: isolation and characterization of the gene. Proc Natl Acad Sci USA 1992;89:1199–1203. [PubMed: 1741374]

Quinn JC, Molinck M, Martynoga BS, Zaki PA, Faedo A, Bulfone A, Hevner RF, West JD, Price DJ. Pax6 controls cerebral cortical cell number by regulating exit from the cell cycle and specifies cortical cell identity by a cell autonomous mechanism. Dev Biol 2007;302:50–65. [PubMed: 16979618]

Russ AP, Wattler S, Colledge WH, Aparicio SA, Carlton MB, Pearce JJ, Barton SC, Surani MA, Ryan K, Nehls MC, et al. Eomesodermin is required for mouse trophoblast development and mesoderm formation. Nature 2000;404:95–99. [PubMed: 10716450]

Sowden JC, Holt JK, Meins M, Smith HK, Bhattacharya SS. Expression of Drosophila omb-related T-box genes in the developing human and mouse neural retina. Invest Ophthalmol Vis Sci 2001;42:3095–3102. [PubMed: 11726608]

Strumpf D, Mao CA, Yamanaka Y, Ralston A, Chawengsaksophak K, Beck F, Rossant J. Cdx2 is required for correct cell fate specification and differentiation of trophectoderm in the mouse blastocyst. Development 2005;132:2093–2102. [PubMed: 15788452]

Su H, Mills AA, Wang X, Bradley A. A targeted X-linked CMV-Cre line. Genesis 2002;32:187–188. [PubMed: 11857817]

Trieu M, Rhee JM, Fedtsova N, Turner EE. Autoregulatory sequences are revealed by complex stability screening of the mouse brn-3.0 locus. J Neurosci 1999;19:6549–6958. [PubMed: 10414983]

Wang SW, Gan L, Martin SE, Klein WH. Abnormal polarization and axon outgrowth in retinal ganglion cells lacking the POU-domain transcription factor Brn-3b. Mol Cell Neurosci 2000;16:141–156. [PubMed: 10924257]

Wang SW, Kim BS, Ding K, Wang H, Sun D, Johnson RL, Klein WH, Gan L. Requirement for math5 in the development of retinal ganglion cells. Genes Dev 2001;15:24–29. [PubMed: 11156601]

Wang TF, Ding CN, Wang GS, Luo SC, Lin YL, Ruan T, Rubenstein JL, Heueh YP. Identification of Tbr-1/CASK complex target genes in neurons. J Neurochem 2004;91:1483–1492. [PubMed: 15584924]

Waxman, SG.; Kocsis, JD.; Black, JA. Pathophysiology of demyelinated axons. In: Waxman, SG.; Kocsis, JD.; Stys, PK., editors. The Axon: Structure, Function and Pathophysiology. New York: Oxford University Press; 1995. p. 438-461.

Wells J, Farnham PJ. Characterizing transcription factor binding sites using formaldehyde crosslinking and immunoprecipitation. Methods 2002;26:48–56. [PubMed: 12054904]

Xiang M, Zhou L, Macke JP, Yoshioka T, Hendry SH, Eddy RL, Shows TB, Nathans J. The Brn-3 family of POU domain factors: primary structure, binding specificity, and expression in subsets of retinal ganglion cells and somatosensory neurons. J Neurosci 1995;15:4762–4785. [PubMed: 7623109]

Young RW. Cell differentiation in the retina of the mouse. Anat Rev 1985a;212:199–205.

Young RW. Cell proliferation during postnatal development of the retina in the mouse. Brain Res 1985b; 353:229–239. [PubMed: 4041905]

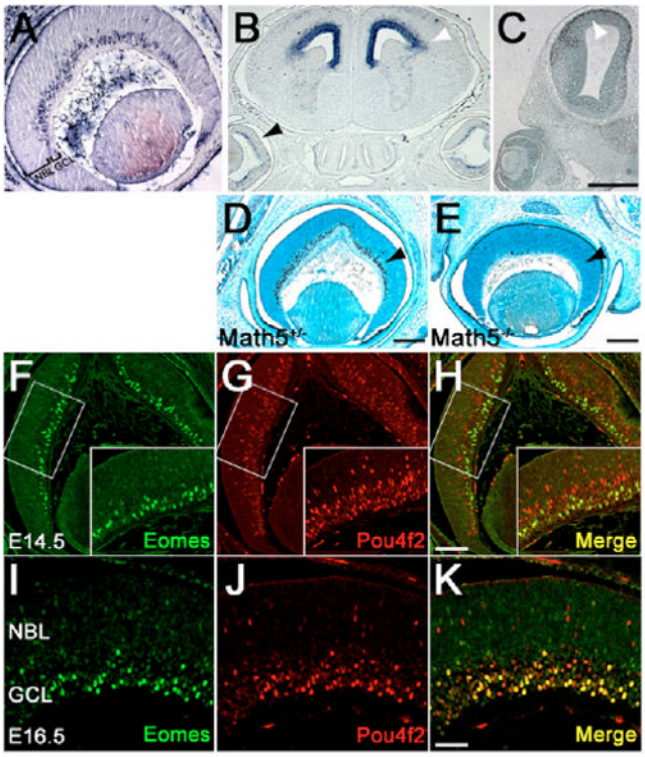

Fig. 1. *Eomes* expression in the developing retina

Retinal sections from the indicated developmental stages were labeled with an *Eomes* antisense probe (**A,B**) or anti-Eomes antibody (**C-K**). *Eomes* expression starts at E14.5 in the innermost layer of developing retina (A). At E16.5, *Eomes* expression is mainly localized in the same area (B, black arrowhead) and in the forebrain (white arrowhead). At E13.5, although Eomes expression is detected in the developing forebrain (C, arrowhead), it is undetectable in the retina. (D,E) In *Math5*$^{+/-}$ retinas (D), Eomes is detected in the GCL (strongly) and NBL (weakly), but in *Math5*$^{-/-}$ retinas (E), Eomes expression in GCL is undetectable. (F-H) At E14.5, Pou4f2 and Eomes colocalize in RGCs in the innermost layer. Developing RGCs in the NBL with strong Pou4f2 expression are Eomes negative. Weak Eomes expression can be detected in the NBL at E14.5. (I-K) At E16.5, expression of Pou4f2 and Eomes is largely restricted to the GCL. Scale bars: 500 μm in C; 200 μm in D,E; in H, 100 μm for F-H; in K, 50 μm for I-K.

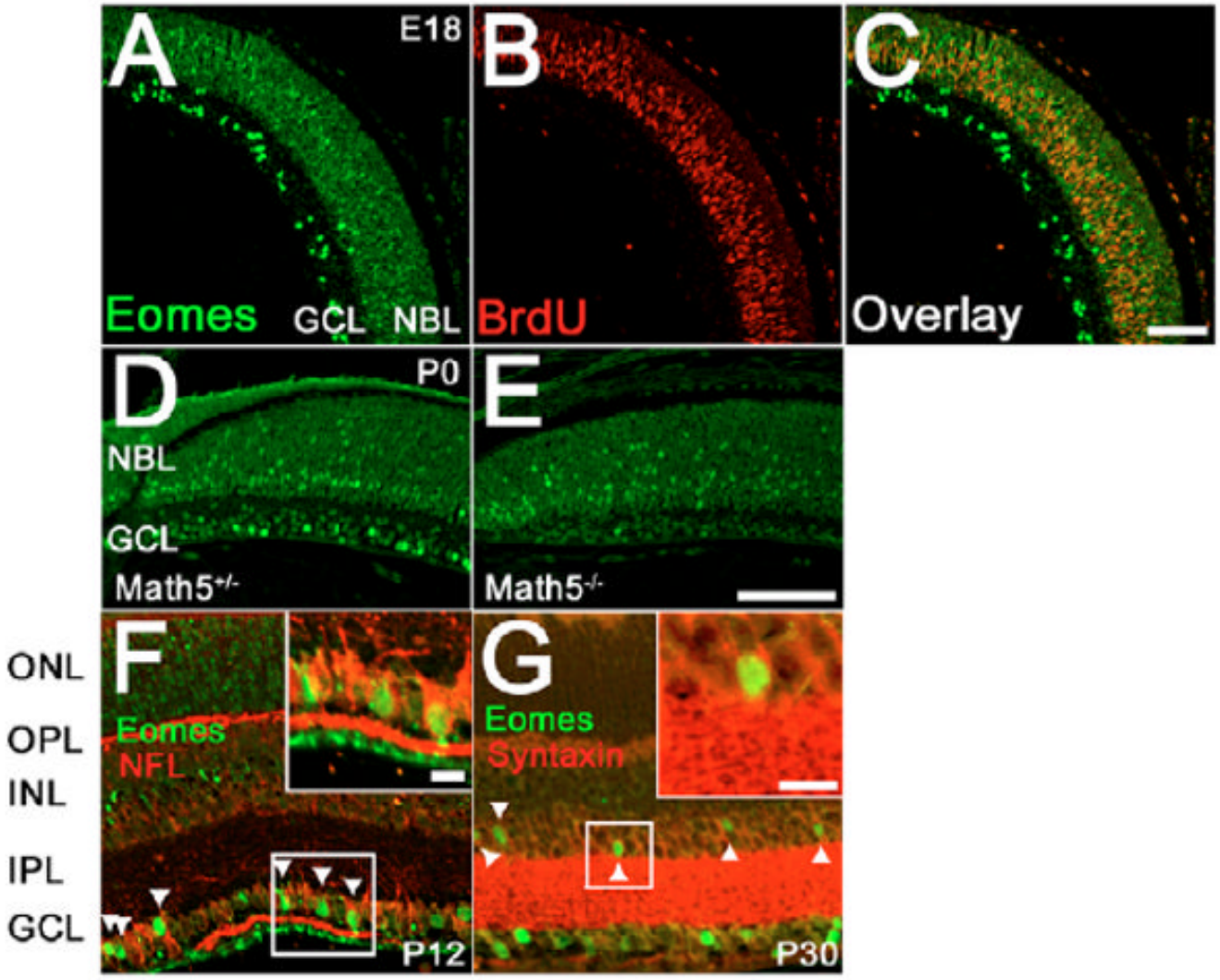

Fig. 2. *Eomes* expression in the NBL

(**A-C**) An E18 retina pulse-labeled with BrdU: anti-Eomes (A), anti-BrdU (B) and merged image (C). (**D**) At P0 in *Math5*$^{+/-}$ retinas, Eomes is expressed in the GCL and NBL. (**E**) At P0 in *Math5*$^{-/-}$ retinas, much of the Eomes expression is absent from the GCL but not the NBL. (**F**) At P12, some Eomes-positive cells in the GCL co-localize with NFL (arrowheads). Eomes is expressed in the nucleus and NFL is expressed in the cytoplasm. (**G**) At P30, Eomes is expressed in the GCL and in a subset of amacrine cells that are co-labeled with syntaxin (arrowheads). Syntaxin expression is cytoplasmic. The boxed region in the inset is enlarged to emphasize the co-localization of nuclear Eomes and cytoplasmic syntaxin expression. Scale bars: in C, 100 μm for A-C; in E, 100 μm for D,E; 10 μm in insets in F,G.

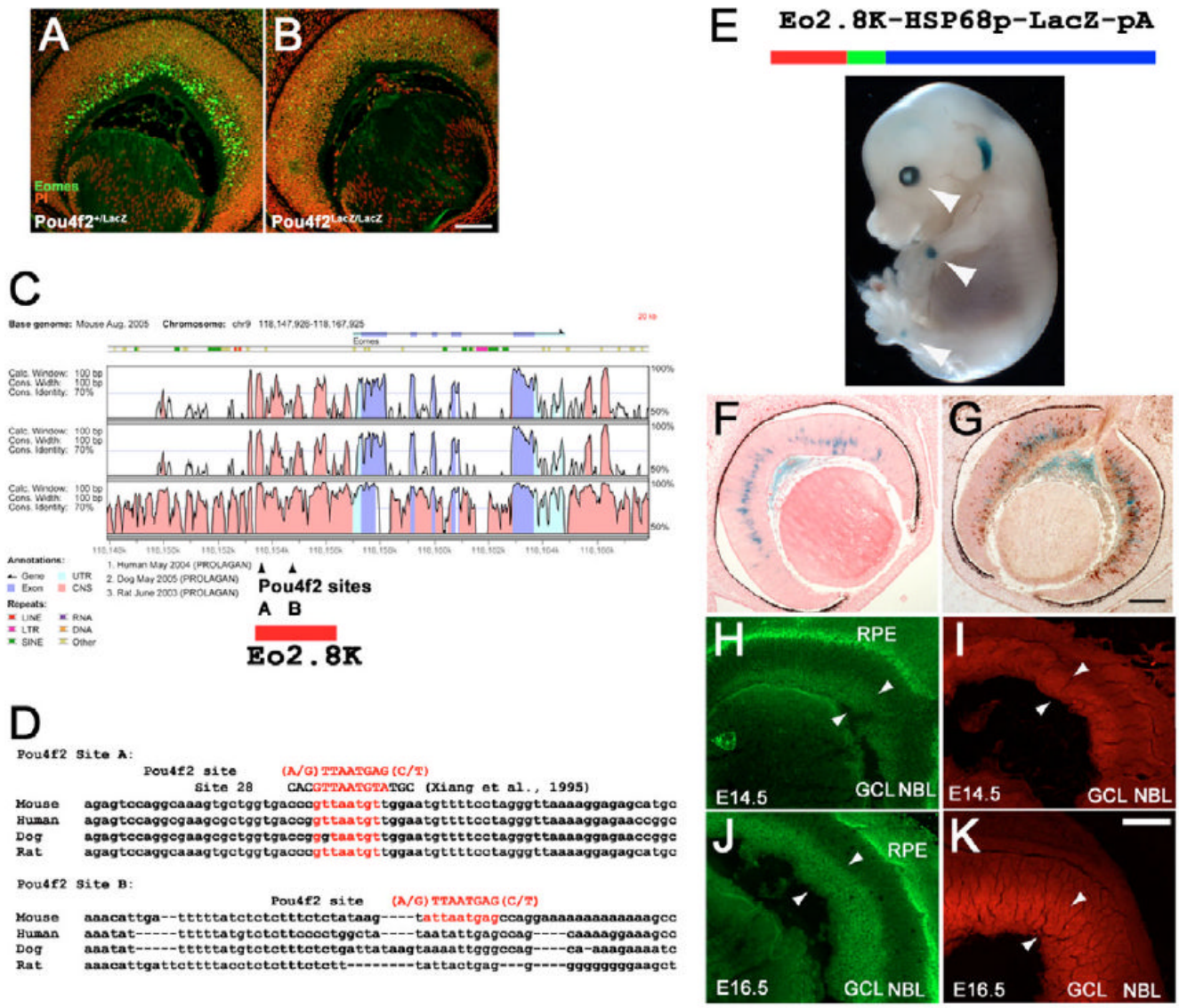

Fig. 3. Identification of an upstream *Eomes* retinal enhancer containing Pou4f2-binding sites

(**A,B**) E14.5 retinal sections from *Pou4f2*$^{+/lacZ}$ and *Pou4f4*$^{lacZ/lacZ}$ embryos immunostained with anti-Eomes antibody and counterstained with propidium iodide. (**C**) 20 kb Vista analysis of *Eomes* comparing mouse, human, dog and rat genomes. Pou4f2-binding sites A and B are indicated by arrowheads. (**D**) The DNA sequence of Pou4f2 sites A and B. The 2.8 kb retinal enhancer fragment is indicated in red. (**E**) Transgenic embryos carrying Eo2.8k-HSP68p-LacZ-pA construct stain positively in the retina and limb (arrowheads). (**F**) Histological retinal section of Eo2.8k-HSP68p-LacZ-pA E14.5 embryos shows *lacZ* expression in RGCs within the NBL. *lacZ*-expressing cells co-localized with Pou4f2-expressing cells, detected using anti-Pou4f2 antibody (**G**). (**H-K**) GFP expression in Bac Eomes::GFP retinas. GFP fluorescence in retinas from E14.5 (H) and E16.5 (J) embryos. There is intense auto-fluorescence in retina pigment epithelia layer (RPE). Immunostaining using Alexa-555-anti-GFP antibody on retinal sections from E14.5 (I) and E16.5 (K) embryos. Scale bars: 100 μm in B,G,K for A,B, F,G and H-K, respectively.

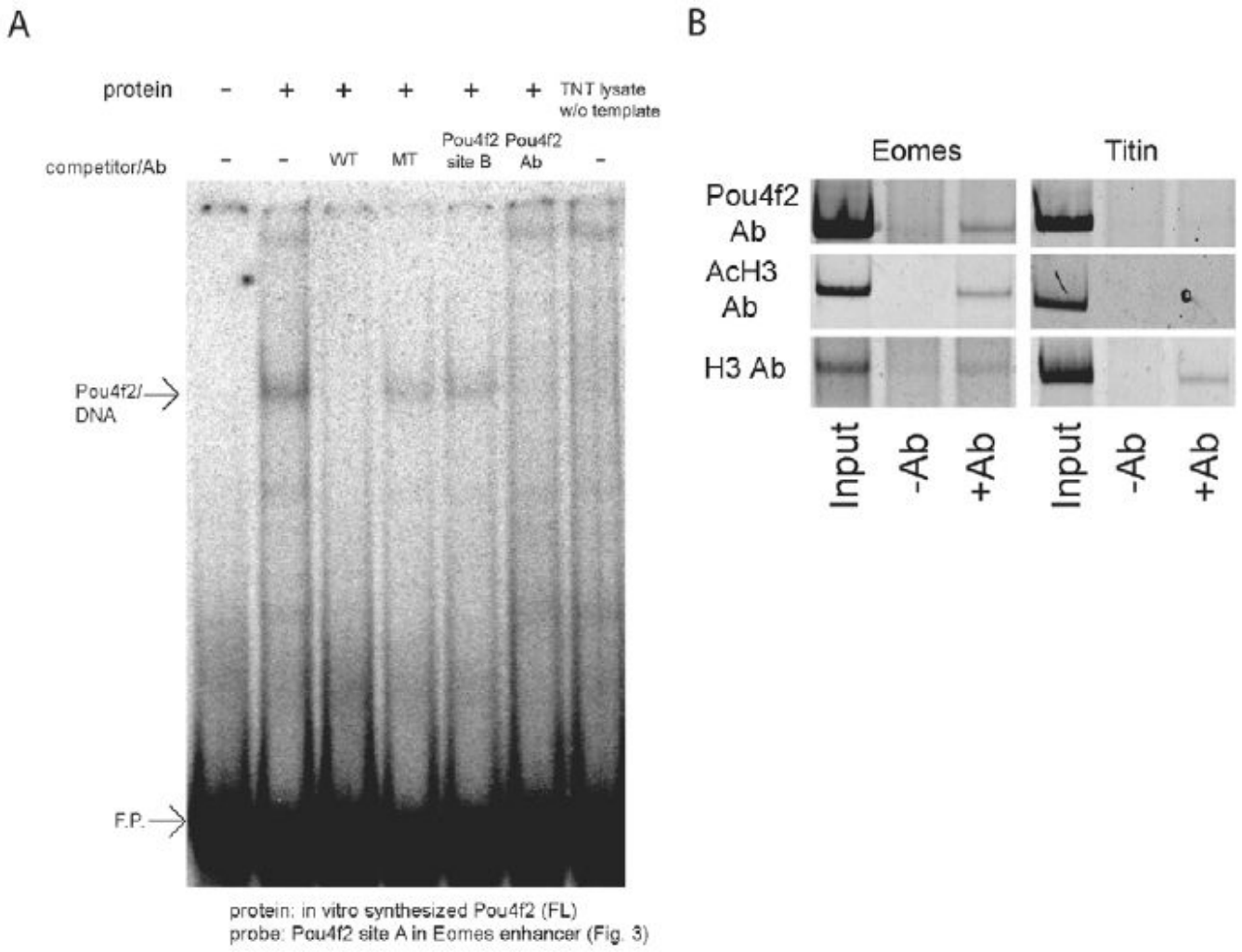

Fig. 4. EMSA and ChIP of Pou4f2-binding to site A within the *Eomes* retinal enhancer

(**A**) Pou4f2 binds to site A in vitro. A probe containing Pou4f2-binding site A forms a Pou4f2-DNA complex. The left-most lane shows the free probe (F.P.). The second lane shows the Pou4f2-DNA complex formed in the presence of in vitro-synthesized Pou4f2. Free probe and complex are indicated by arrows. The remaining lanes show the extent of complex formation in the presence of a 500-fold molar excess of wild-type (WT) and mutated (MT) site A oligonucleotides, site B oligonucleotide, and anti- Pou4f2 antibody. (**B**) ChIP analysis using retinas from E15.5 embryos shows occupancy of Pou4f2 at site A. Sequences around Eomes site A or Titin were amplified after immunoprecipitation with anti-Pou4f2/Brn3b, anti-acetylated-histone H3 or anti-histone H3 antibodies. The left lanes show the expected size of the amplified products generated using input chromatin extracts. The right lanes show the amplified products resulting from the immunoprecipitation of chromatin extracts. The middle lanes show the amplified products generated using mock immunoprecipitation of chromatin extracts without the primary antibody.

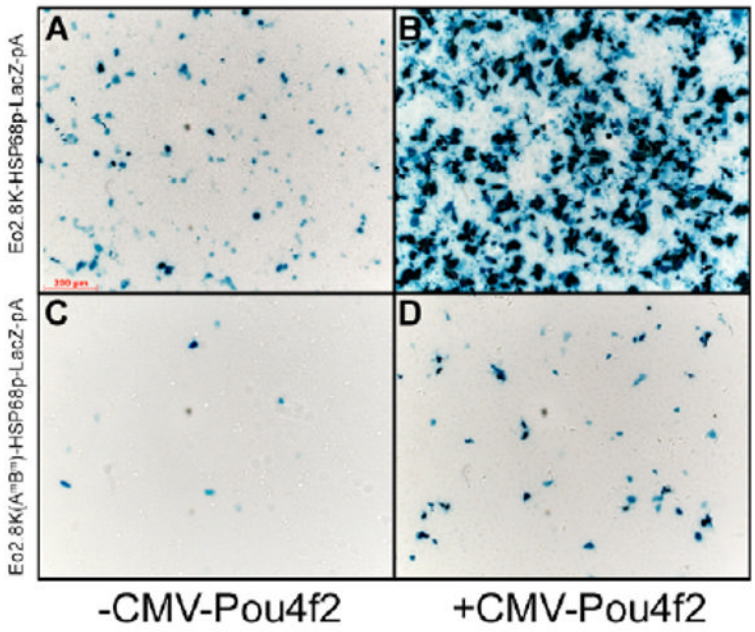

Fig. 5. Transcriptional activity of the upstream *Eomes* retinal enhancer

U2OS cells were transfected using Eo2.8k-HSP68p-LacZ-pA (**A,B**) or Eo2.8k (A^mB^m)-HSP68p-LacZ-pA plasmid (**C,D**) without (A,C) or with (B,D) CMV-Pou4f2 plasmid. Scale bar: 200 μm.

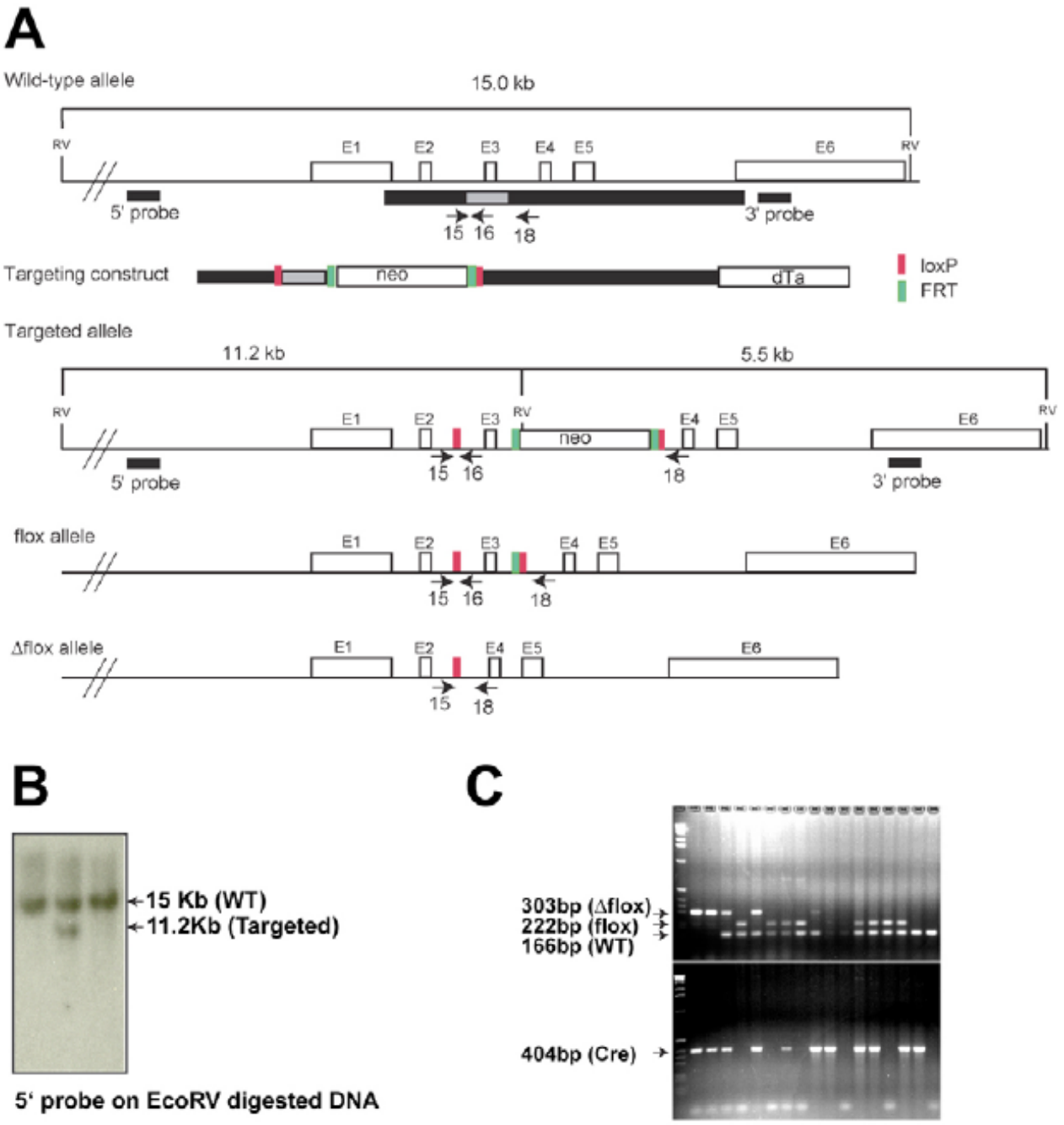

Fig. 6. Generation of a floxed conditional *Eomes* allele and creation of *Eomes*$^{flox/flox}$ mice

(**A**) Genomic structure of *Eomes*, the targeting construct, the targeted *Eomes* allele (*Eomes*^{flox}) and the deleted allele (*Eomes*$^{\Delta flox}$). Exons are designated as E1-E6. The black and gray bars indicate the regions that were amplified from genomic DNA to generate the targeting construct. Small arrows below the constructs represent the primers used for PCR genotyping. Red boxes indicate loxP sites, and green bars indicate FRT sites. (**B**) Southern blot analysis of DNA isolated from ES cells. The 5′ probe recognizes 15 kb wild-type and 11.2 kb targeted *EcoRV* fragments. A targeted ES cell is shown in the middle lane, whereas the left and right lanes are untargeted ES cells. (**C**) Representative PCR genotyping from tail DNA using a three-primer PCR strategy for the different *Eomes* alleles and *Cre* transgene. The top gel represents

Eomes allele genotyping, and the bottom gel shows the presence of the *Cre* transgene. In the top gel, the arrows from top to bottom indicate products amplified from primers 15/18 (303 bp for Δflox), 15/16 (222 bp for flox) and 15/16 (166 bp for wild-type), respectively. The 303 bp fragment for the Δflox allele was often preferentially amplified (lanes 1, 2, 3, 5 and 9) from the tail DNA because of leaky expression from the *Six3-Cre* transgene.

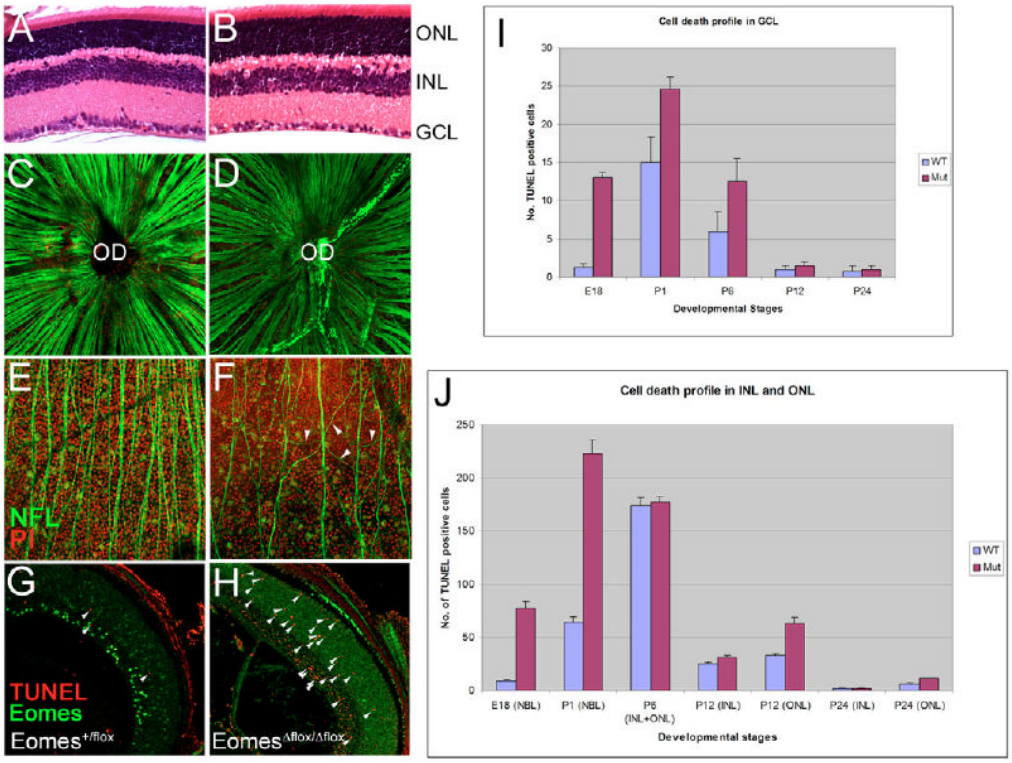

Fig. 7. Reduced numbers of RGCs and RGC axons and cell death in *Eomes*$^{\Delta flox/\Delta flox}$ mice

(**A**,**B**) Retinal sections from *Eomes*$^{+/flox}$ (A) and *Eomes*$^{\Delta flox/\Delta flox}$ (B) retinas at P24 were stained with Hematoxylin and Eosin. (**C-F**) Immunostaining using anti-NFL antibody on flat-mount *Eomes*$^{+/flox}$ (C,E) and *Eomes*$^{\Delta flox/\Delta flox}$ (D,F) retinas. NFL staining in the central region of the *Eomes*$^{\Delta flox/\Delta flox}$ retina is less intense and sparser than in the *Eomes*$^{+/flox}$ control retina (C,D). The difference is more noticeable in the peripheral region (E,F). Many axons are oriented aberrantly (F, arrowheads). OD, optical disc. (**G,H**) Representative cell death pattern at E18. In *Eomes*$^{\Delta flox/\Delta flox}$ retinas (H), massive cell death can be detected while *Eomes*$^{+/flox}$ control retinas show little cell death (G). (**I,J**) Cell death profile from E18 to P24 in the GCL (I), and in the INL and ONL (J).

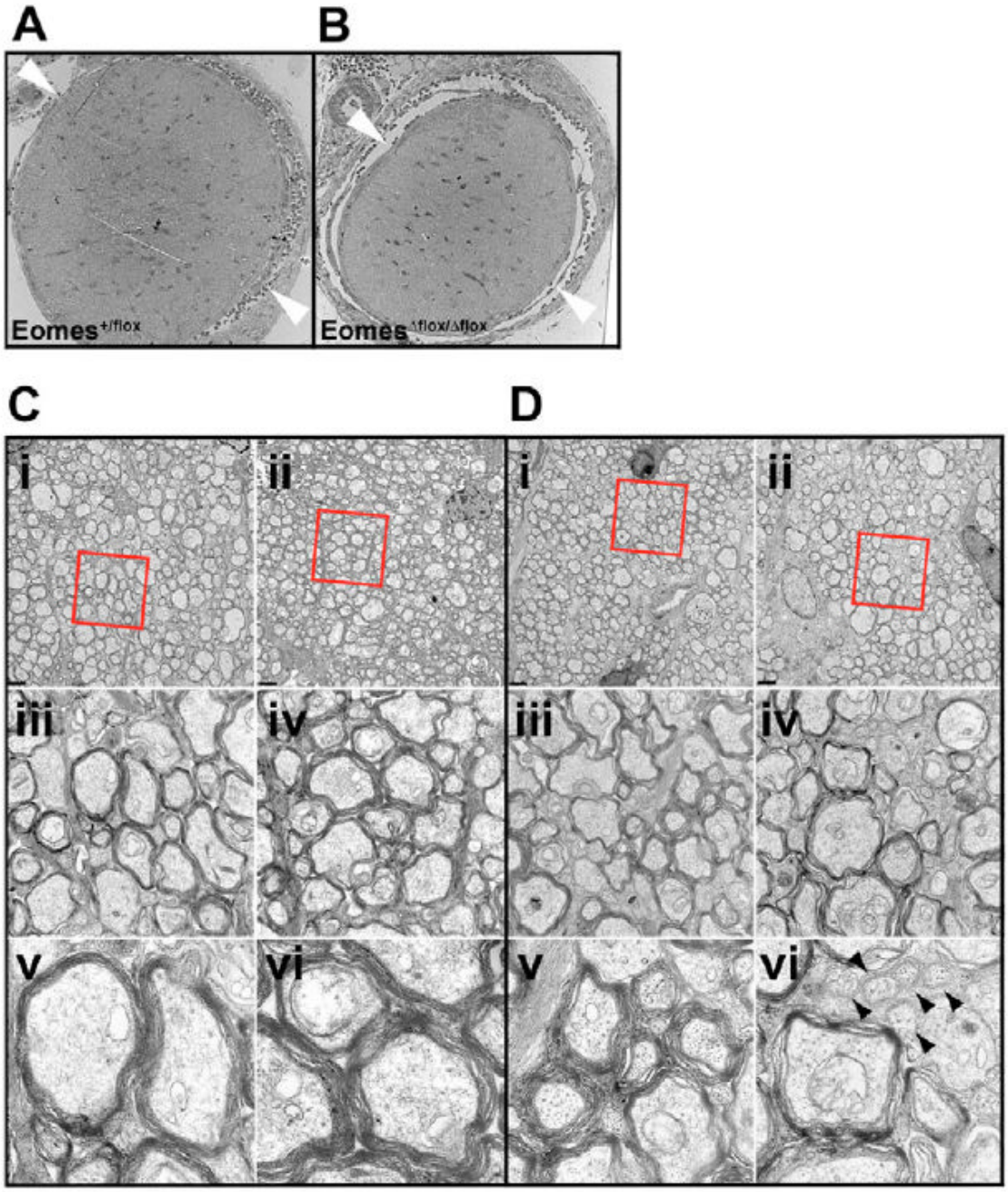

Fig. 8. Defects in optic nerve development and myelin ensheathment in *Eomes*$^{\Delta flox/\Delta flox}$ mice

(**A**,**B**) Low-magnification images of cross-sections of optic nerves from *Eomes*$^{+/flox}$ (A) or *Eomes*$^{\Delta flox/\Delta flox}$ (B) P30 mice. Arrowheads indicate the size of the optic nerve. (**C,D**) Higher magnification images of cross-sections of optic nerves from *Eomes*$^{+/flox}$ (C) and *Eomes*$^{\Delta flox/\Delta flox}$ (D) P30 mice. Arrowheads in D, part vi point to abnormal neurites. Each row in C and D represents a higher magnification. Scale bars: 2 μm in C,D, parts i.